Inelastic neutron scattering studies of phonon spectra, and simulations of pressure-induced amorphization in tungstates AWO_4 (A = Ba, Sr, Ca, and Pb)

Prabhatasree Goel,[1] M. K. Gupta,[1] R. Mittal,[1] S. Rols,[2] S. N. Achary,[3] A. K. Tyagi,[3] and S. L. Chaplot[1]

[1]*Solid State Physics Division, Bhabha Atomic Research Centre, Mumbai 400085, India*

[2]*Institut Laue-Langevin, BP 156, 38042 Grenoble Cedex 9, France*

[3]*Chemistry Division, Bhabha Atomic Research Centre, Mumbai 400085, India*

(Received 25 July 2014; revised manuscript received 2 March 2015; published 17 March 2015)

Lattice dynamics and high-pressure phase transitions in AWO_4 (A = Ba, Sr, Ca, and Pb) have been investigated using inelastic neutron scattering experiments, *ab initio* density functional theory calculations, and extensive molecular dynamics simulations. The vibrational modes that are internal to WO_4 tetrahedra occur at the highest energies consistent with the relative stability of WO_4 tetrahedra. The neutron data and the *ab initio* calculations are found to be in excellent agreement. The neutron and structural data are used to develop and validate an interatomic potential model. The model is used for classical molecular dynamics simulations to study their response to high pressure. We have calculated the enthalpies of the scheelite and fergusonite phases as a function of pressure, which confirms that the scheelite to fergusonite transition is second order in nature. With increase in pressure, there is a gradual change in the AO_8 polyhedra, while there is no apparent change in the WO_4 tetrahedra. We found that all the four tungstates amorphize at high pressure. This is in good agreement with available experimental observations which show amorphization at around 45 GPa in $BaWO_4$ and 40 GPa in $CaWO_4$. Further molecular dynamics simulations at high pressure and high temperature indicate that application of pressure at higher temperature hastens the process of amorphization. On amorphization, there is an abrupt increase in the coordination of the W atom while the bisdisphenoids around the A atom are considerably distorted. The pair-correlation functions of the various atom pairs corroborate these observations. Our observations aid in predicting the pressure of amorphization in $SrWO_4$ and $PbWO_4$.

DOI: 10.1103/PhysRevB.91.094304 PACS number(s): 64.60.−i, 63.20.dk

I. INTRODUCTION

Compounds of the form MWO_4 (M = Mn, Cu, Ba, Sr, etc.) are studied [1–11] extensively for their interesting properties and usefulness. In this paper we report lattice vibrational studies on AWO_4 type tungstates with A = Ba, Sr, Ca, and Pb, which are important for their scientific and technological applications [12–18]. These compounds in nano or bulk state find applications in solid-state scintillators [16–19], optoelectronic devices, solid-state laser applications, etc., as well as in understanding of geological aspects. They also form a part of oxide ceramic composites useful for cryogenic detectors. These possible applications have motivated extensive interest in understanding the fundamental physical properties [20–31] of the AWO_4 tungstates.

The compounds under normal conditions crystallize in the tetragonal scheelite [28] structure ($CaWO_4$ mineral structure). The scheelite structure (space group 88, $Z = 4$) adopted by AWO_4 has a body centered unit cell, with A atoms occupying S_4 symmetry while the sixteen oxygen atoms occupy C_1 sites. Each W is surrounded by four equivalent oxygen atoms in a tetrahedral symmetry and A is surrounded by eight oxygen atoms. Along the a axis the WO_4 units are directly aligned whereas along the c axis, AO_8 dodecahedra are interspersed between two WO_4 tetrahedra. Hence, different arrangement of hard WO_4 tetrahedra along the c and a axes accounts for the difference in compressibility of the two unit-cell axes. These compounds exhibit a rich phase diagram with respect to change in pressure and temperature [23]. Several experimental and theoretical efforts have been undertaken to obtain understanding of the phase diagram of the compounds [20–27], which still remains elusive. Extensive Raman [27–29] and infrared [30] scattering techniques have been used to study the zone-center phonon modes in several of these tungstates. Experimental studies using angle dispersive x-ray diffraction (ADXRD) and x-ray absorption near-edge structure measurements (XANES) have observed that upon compression at high pressures AWO_4 undergoes a scheelite to fergusonite phase transition at room temperature. This transformation is displacive in nature [23]. The β angle of the high-pressure monoclinic cell of the fergusonite phase is only a little different from 90°. Upon further compression the compounds change into denser monoclinic and orthorhombic phases, before amorphizing. In the meanwhile, experiments like Raman scattering suggest [27–29] that there is a possibility of a reconstructive, first-order transition to $P2_1/n$ phase which coexists with the fergusonite phase. However, this competing phase is kinetically hindered.

The earlier diffraction experiments and *ab initio* studies [23,24] surmise that orthotungstates and other related ABX_4 compounds (e.g., $YLiF_4$ and $BiVO_4$) exhibit a systematic trend in their structural sequence: zircon → scheelite → fergusonite → denser monoclinic phases → orthorhombic phases. Our calculations of the zone-center modes and equation of state are in agreement with the previous [23–30] calculations as well as experimental data.

Preliminary results of inelastic neutron scattering measurements on $SrWO_4$ and theoretical studies on $SrWO_4$ and $BaWO_4$ have been communicated by us in conference proceedings [32]. Herein we report complete and comparative details of the inelastic scattering experiments and theoretical studies on a series of tungstates as AWO_4 (A = Ba, Sr, Ca, and Pb). The measurement of phonons density of states is carried

out by using neutron inelastic scattering. The transferable interatomic potential has been developed and further used in molecular dynamics studies to understand the mechanism of pressure-driven phase changes of AWO_4 (A = Ba, Ca, Sr, and Pb). We have looked at the changes occurring in the lattice under increasing pressure. The simulations have enabled us to understand the behavior of various polyhedra under compression.

II. EXPERIMENTAL DETAILS

Polycrystalline samples of the AWO_4 (A = Ba, Sr, and Ca) were prepared by solid-state reaction of appropriate amounts of alkaline earth carbonate (ACO_3) and WO_3. $CaCO_3$ (Sigma-Aldrich, 99.0%), $SrCO_3$ (Sigma-Aldrich, 99.9%), $BaCO_3$ (Sigma-Aldrich, 99%), and WO_3 (Loba Chemical, 99.8%) were used for this preparation. Both $SrCO_3$ and $BaCO_3$ were heated at 500 °C for 5 h while $CaCO_3$ was heated at 200 °C overnight to remove any adsorbed moisture. WO_3 was heated at 700 °C for 12 h in air before using for the reaction. Pellets of a homogeneous mixture of the appropriate amount of reactants were heated at 900 °C for 24 h in air. The product obtained was rehomogenized and pelletized and then heated at 1200 °C for 24 h. The final products were characterized by powder x-ray diffraction study. All three samples show typical reflections attributable to the scheelite type structure. $PbWO_4$ was prepared by heating the precipitates obtained from $Pb(NO_3)_2$ and Na_2WO_4-$2H_2O$ solutions. $Pb(NO_3)_2$ (Sigma, Aldrich, 99.5%) and Na_2WO_4-$2H_2O$ (Sigma-Aldrich, 99%) were dissolved separately in de-ionized water. Addition of the solution of Na_2WO_4-$2H_2O$ to that of solution of $Pb(NO_3)_2$ leads to the formation of thick white precipitate. The precipitate was washed several times with distilled water to remove all the Na^+ and NO^{3-} ions. Finally the precipitate was dried at room temperature and then slowly heated at 900 °C for 24 h. The product was then rehomogenized, pelletized, and then heated at 1200 °C for 24 h. Formation of crystalline scheelite type $PbWO_4$ was confirmed from the powder XRD data.

The phonon density of states measurements of all AWO_4 (A = Ba, Sr, Ca, Pb) were performed in the neutron-energy gain mode with incident neutron energy of 14.2 meV. The data were taken over the scattering angle 10° to 113°. The signal is corrected for the contributions from the empty cell and suitably averaged over the angular range using the available software package at Institut Laue-Langevin (ILL). The incoherent approximation [33] was used in the data analysis. The data were suitably averaged over the angular range of scattering using the available software package at ILL to obtain the neutron-cross-section weighted phonon density of states. The multiphonon contribution has been calculated using the Sjolander [34] formalism and subtracted from the experimental data.

III. THEORETICAL FORMALISM

Ab initio calculations were performed using the projector-augmented wave (PAW) formalism of the Kohn-Sham density functional theory (DFT) at the generalized gradient approximation (GGA) level formulated by the Perdew-Burke-Ernzerhof (PBE) density functional [35–37]. We have used the Vienna *Ab initio* Simulation Package (VASP) for calculation of total energy and force [38,39]. The force constants have been calculated using the supercell approach implemented in the PHONON package [40], which are further used for calculation of phonon frequencies in the entire Brillouin zone. The total energy calculation has been done on 14 different configurations generated by displacement of symmetry-inequivalent atoms along different Cartesian directions ($\pm x$, $\pm y$, $\pm z$). The kinetic energy cutoff for total energy calculations is 860 eV for all four compounds.

We have used a transferable interatomic potential to study the vibrational properties of the tungstates using lattice dynamics calculations. An interatomic potential [41–43] consisting of short-range and Coulombic terms is used. The parameters of the potentials satisfy the conditions of static and dynamic equilibrium. The calculations have been carried out using the current version of the DISPR [44] software. The radii parameters for M atoms are $r_{Ca} = 2.06$ Å, $r_{Ba} = 2.4$ Å, $r_{Pb} = 2.25$ Å, and $r_{Sr} = 2$ Å, respectively. The parameters of the WO_4 stretching potential are $D = 3.2$ eV, $r_o = 1.75$ Å, and $n = 26.2$ Å^{-1}. The van der Waals interaction between O-O pairs is 80 eV Å^6. The polarizability of the oxygen and alkali earth atoms has been considered in the framework of shell model [43] with shell charge and shell core force constants for oxygen atoms as -2.0 and 50 eV/Å^2 and for alkaline atoms as 3.0 and 50 eV/Å^2, respectively. Molecular dynamics (MD) simulations have been carried out using the model parameters obtained from the lattice dynamics calculations. A super cell consisting of $8 \times 8 \times 4$ unit cells (6144 atoms) has been used to study the response of the compounds on compression. The rigid ion model has been used in the MD simulations. Calculations have been carried out from ambient pressure to around 50 GPa at room temperature, 500, 600, and 700 K. The equation of state has been integrated for about 1400 ps using a time step of 0.002 ps. All the calculations have been done using the lattice and molecular dynamics softwares [44] DISPR and MOLDY developed at Trombay, Mumbai.

IV. RESULTS AND DISCUSSION

The neutron inelastic scattering experiments have been performed using powder samples of the AWO_4 (A = Ba, Sr, Ca, and Pb) at ambient conditions. The measurements have been carried out on the time-of-flight (TOF) instrument IN4C, ILL, Grenoble. The measured phonon density of states of the four tungstates in comparison with *ab initio* and potential model calculations are given in Fig. 1. The potential model calculation results (Fig. 1) are in good agreement with the inelastic neutron data and *ab initio* calculations. This has allowed validation of our model, which is further used to explore the phase stability of the compounds using molecular dynamics simulations as discussed below. The measured spectra show that phonons occur in two distinct regions in these compounds. The first region extends from 0 to 60 meV, while there is another region between 90 and 120 meV. The higher-energy component corresponds to the internal vibrations of the WO_4 tetrahedra.

The *ab initio* calculated partial phonon densities of each atom of AWO_4 compounds are given in Fig. 2. It can be seen that the contribution from the A atoms extends up to 20

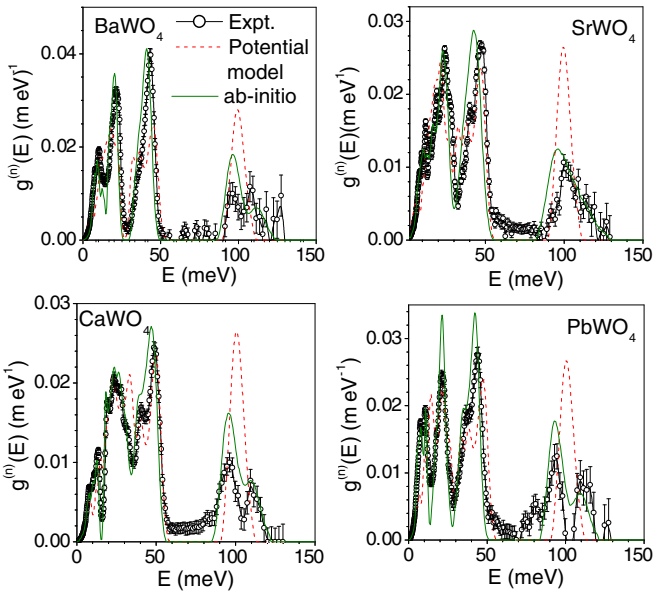

FIG. 1. (Color online) Neutron inelastic scattering data of the phonon density of states in AWO_4 (A = Ba, Ca, Sr, and Pb) compared with our *ab initio* and shell model calculations. The calculated spectra have been convoluted with a Gaussian of full width at half maximum (FWHM) of 10% of the energy transfer in order to describe the effect of energy resolution in the experiment.

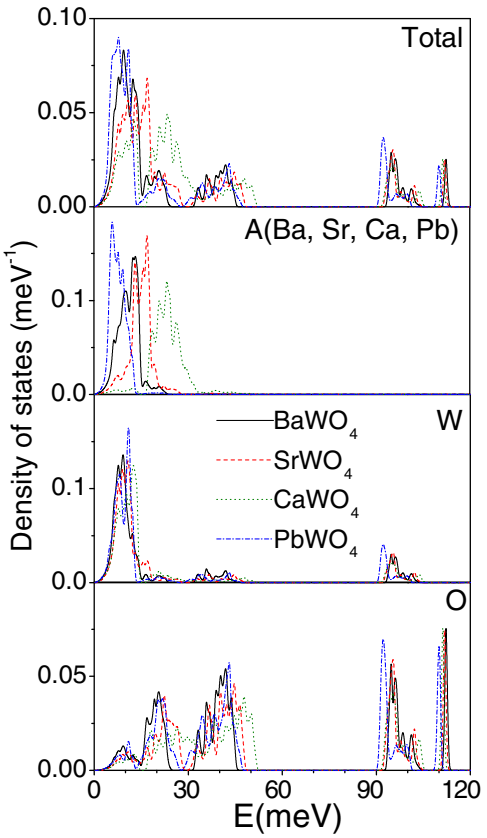

FIG. 2. (Color online) *Ab initio* calculated partial densities of the constituent atoms in AWO_4 (A = Ba, Sr, Ca, and Pb).

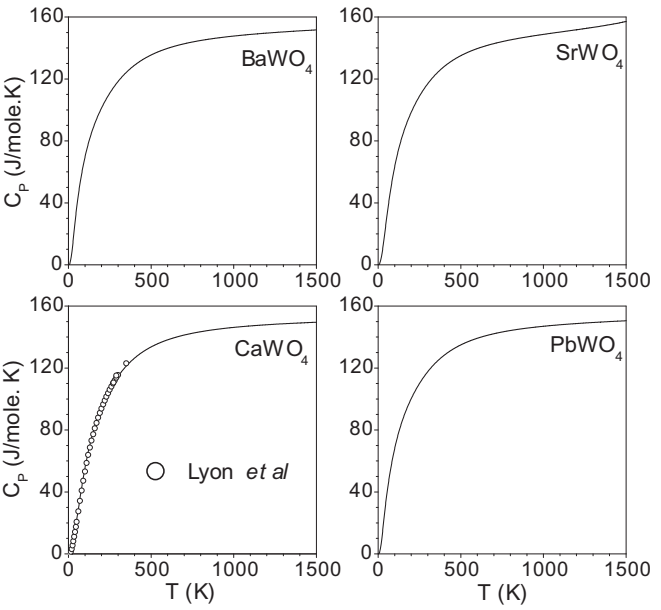

FIG. 3. Experimental and computed (using potential model) specific heat in AWO_4 (A = Ba, Sr, Ca, and Pb). The experimental data for $CaWO_4$ are from Ref. [44].

meV. The contribution of Pb atom is at the lowest energy while that of Ca is at the highest energy, following their respective masses. This is in accordance to their relative atomic mass. The contribution from W atoms is confined within 20 meV, with a very small contribution up to 60 meV. There is another contribution above 90 meV in the band between 90 and

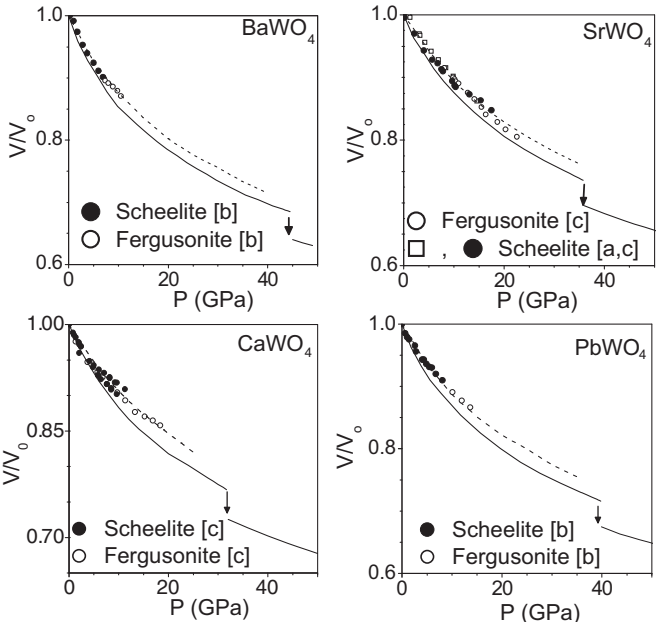

FIG. 4. Calculated (using potential model) and experimental equation of state of AWO_4 (A = Ba, Ca, Sr, and Pb). V and V_o are the unit-cell volume at high and ambient pressure, respectively. [a], [b], and [c] correspond to the experimental data from Refs. [13,24,27]. The full and dashed lines correspond to calculations at T = 300 K and 0 K, respectively.

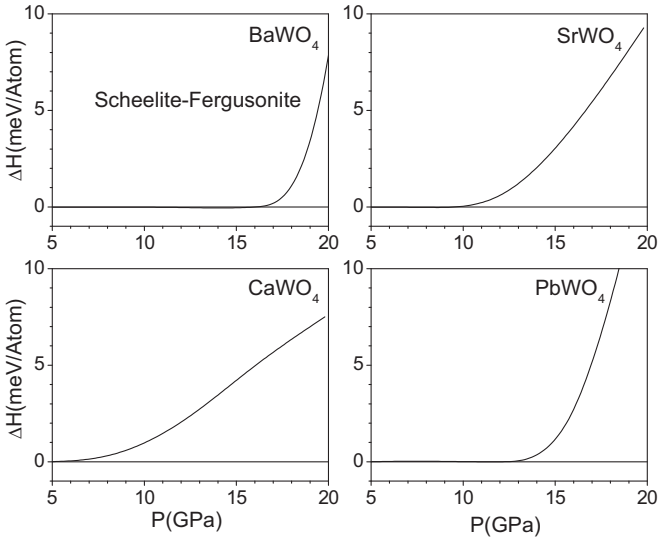

FIG. 5. Difference in enthalpy ($\Delta H = H_S$-H_F) with increasing pressure for the scheelite and fergusonite phases in all four AWO_4 (A = Ba, Ca, Sr, and Pb) compounds as computed from *ab initio* studies.

120 meV from W atoms. In the case of oxygen, the contribution is in the complete range 0–60 meV and in the band between 90 and 120 meV. The partial phonon densities ascertain that the contribution above 90 meV in the measured spectra is from the internal stretching modes of the W-O tetrahedra. The computed density of states has been used to determine the specific heat capacity of the four oxides as shown in Fig. 3. The available data on $CaWO_4$ [45] have been compared and found to be in very good agreement with our calculated data.

Using the interatomic potential developed, we have studied the pressure evolution of the tungstates. Figure 4 gives the equation of state of the four compounds. These compounds are found to undergo initial transformation from scheelite ($I4_1/a$) to fergusonite ($I2/a$). According to experimental XANES [23,24] and ADXRD [23,24] studies, it is now well known that $BaWO_4$ transforms from the scheelite to fergusonite phase at 7.5 GPa, $PbWO_4$ transforms at 9 GPa, $CaWO_4$ undergoes the above-said transition at 11 GPa, and $SrWO_4$ at 10 GPa. The pressure-driven transition to the fergusonite phase is of displacive nature; it is known to be a second-order phase transition with almost no discernible volume discontinuity.

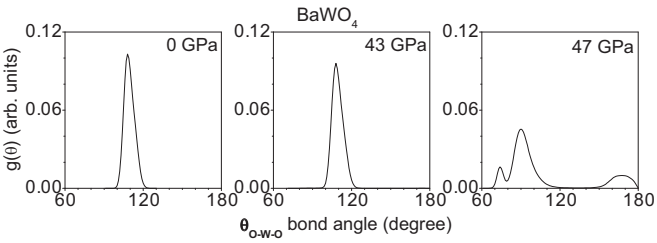

FIG. 7. Intratetrahedral bond angle O-W-O with changing pressure at 300 K in $BaWO_4$.

The change in the β angle is only feeble; change in the b lattice parameters is also negligible. This change is not evident from our MD calculations.

Earlier *ab initio* calculations [24,27] involve study of the zone-center phonon modes, equation of state, and total energy (Φ) comparisons between various phases with increasing pressure to study the relative stability of different phases. The authors find that the fergusonite and scheelite phases are energetically very close and indistinguishable. We have carried out enthalpy ($H = \Phi + PV$, where Φ is the total energy) calculations in the two phases. The calculated difference in enthalpy between the scheelite and fergusonite phases is shown in Fig. 5. We can see that difference in the enthalpy of the two phases increases gradually beyond a certain pressure value, which is different for each of the AWO_4's. Our findings are in agreement with previous experimental XANES and ADXRD measurements [23,24,27], that this transition is continuous and second order in nature.

In our molecular dynamics calculations we can see that there is a discontinuity in the pressure-volume curve (Fig. 4), which suggests a change in phase. In case of $CaWO_4$, this change is seen around 30 GPa, around 34 GPa in $SrWO_4$, in case of $PbWO_4$ it is around 38 GPa while in the case of $BaWO_4$ it is around 45 GPa. Detailed studies were done to understand this sudden change in the equation of state. Figure 6 gives the structural arrangement of the different polygons at different pressures (in $BaWO_4$) as obtained from our computations. At $P = 0$ GPa, the atoms are arranged in the scheelite structure; the A atom is in AO_8 coordination while W is in tetrahedral WO_4 coordination. Regions B and C are identified to depict the coordination of A and W atoms. As pressure is increased, at 43 GPa, there is no visible change in the structural arrangement of the various polygons. There is no change in the coordination

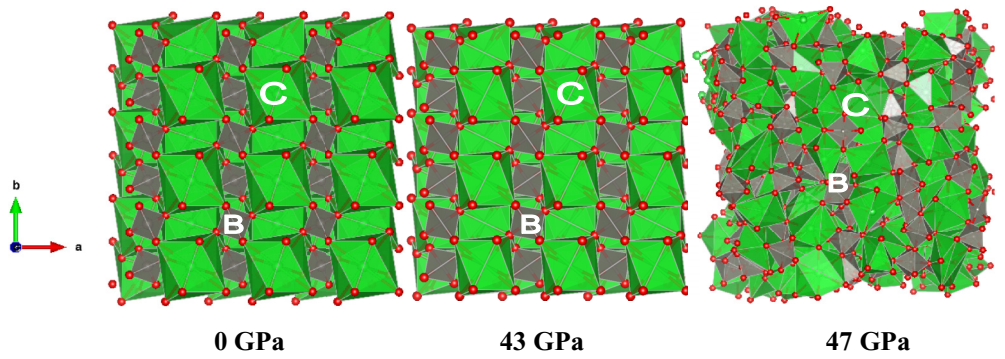

FIG. 6. (Color online) The structure of the $BaWO_4$ supercell evolving under pressure at 300 K. Regions B and C are marked to depict and understand the change in coordination around A and W atoms. (c axis is perpendicular to the plane of the paper).

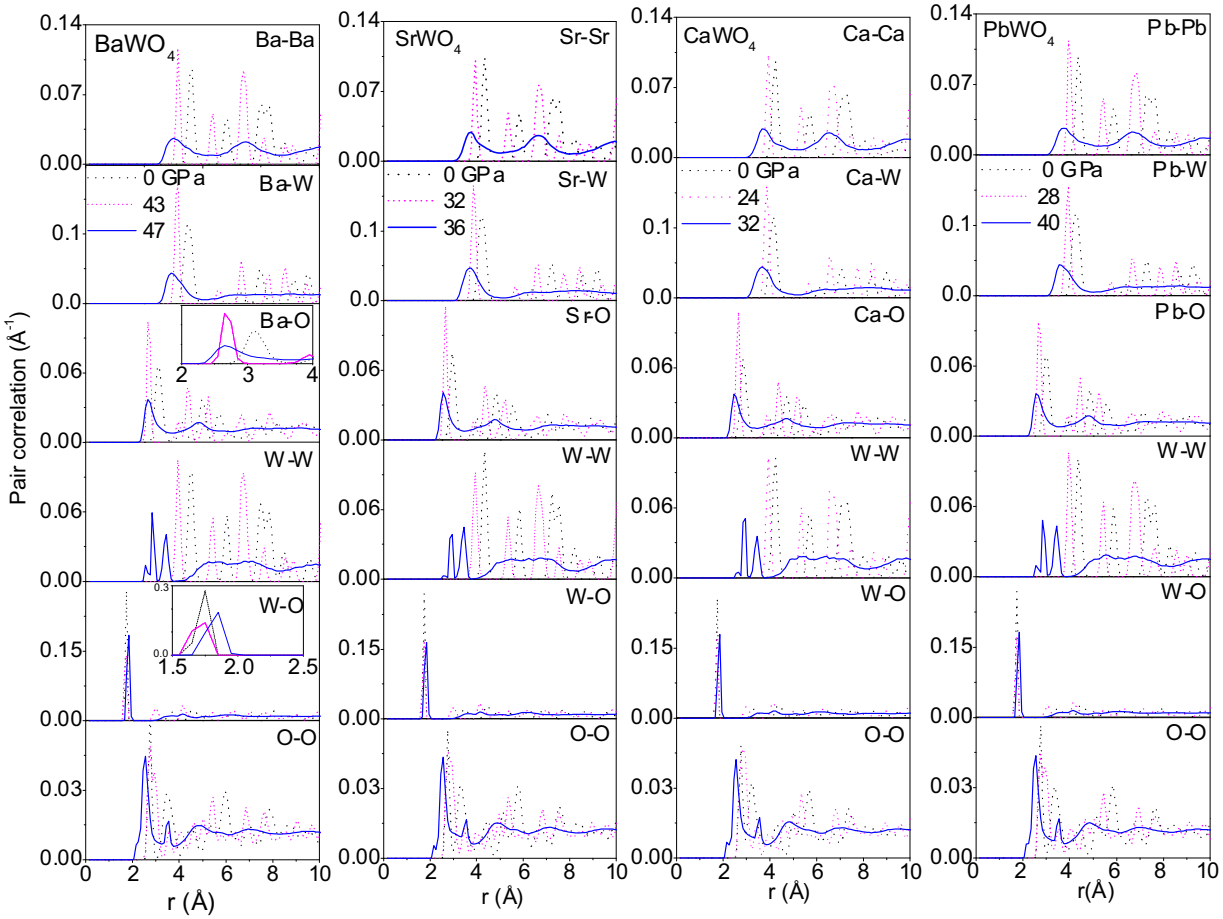

FIG. 8. (Color online) Pair correlations at 300 K between various atomic pairs as obtained from molecular dynamics simulations.

around the *A* and W atoms. Beyond 45 GPa, there is a volume drop in $BaWO_4$. This observation coincides with the volume discontinuity observed around 45 GPa in $BaWO_4$ in Fig. 4. The structure at 47 GPa shows several obvious changes as compared to earlier structures. In region C, it can be seen that *A* atoms are no longer in perfect bisdisphenoids; instead it is now seen in a highly distorted polygon. In region B, W atoms show significant changes; the coordination number has increased. Most of the WO_4 tetrahedra have changed into distorted WO_6.

Further credence to this observation is obtained from the O-W-O bond angle distribution given in Fig. 7. At ambient pressure, all WO_4 tetrahedra are regular with O-W-O angle equal to 109°. At 43 GPa, WO_4 tetrahedra are still regular. But on amorphization, the increase in coordination has resulted in the change in the bond angle. The majority of the O-W-O angle is around 90° which corresponds to an octahedral arrangement. Not all the W's have attained a coordination of 6; hence distortion of the tetrahedra has given rise to a range of angles for the O-W-O bond as seen in Fig. 7. Similar behavior is seen in all the remaining tungstates.

In order to obtain a deeper understanding into this volume discontinuity, we have studied the local order in the lattice between various atomic pairs. The pair correlations have been computed in these compounds with increasing pressure. Figure 8 shows the pair-correlation function between *A*-W, *A*-O, *A*-*A*, W-W, W-O, and O-O at various pressures. We find that with increasing pressure, there are subtle and small changes in the correlations between the different atomic pairs. In the case of $BaWO_4$, the correlations broaden beyond 47 GPa, as seen from the plots in Fig. 8. This is in very good agreement with the reported value [24] of 45 GPa for amorphization in $BaWO_4$. In the case of $CaWO_4$, the broadening of peaks appears around 32 GPa, while the experiments show [28] amorphization around 40 GPa. Our molecular dynamics calculations predict that in the case of $SrWO_4$, at 36 GPa the peaks in the calculated pair correlations broaden, implying that the discrete ordering is lost. In $PbWO_4$, a similar trend is observed at 40 GPa. These observations are in tandem with the equation of states (Fig. 4) computed in each of the compounds.

Careful investigations of the various atomic pairs reveal some interesting observations. In the case of *A*-O pair distribution, we find that changes due to increase in pressure are seen to occur gradually, as can be seen in the inset of the Ba-O pair distribution. There is gradual decrease in the bond length on going from 0 to 43 GPa. The BaO_8 units are able to withstand the increased pressure with gradual rearrangements of the Ba-O bonds, but beyond 43 GPa, the polyhedra distort considerably. This leads to the broadening of peaks, suggesting the loss of long-range order. In the case of WO_4 tetrahedra, there is almost no change in the bond length (changes by about 0.015 Å) as pressure is increased from 0 to 43 GPa

TABLE I. Comparison between the experimental and calculated bulk modulus (B) (in GPa units) and its pressure derivate (B'). The experimental values at 300 K are from Ref. [24]. The B values at 300 K has been obtained using the B' values estimated at 0 K.

	$BaWO_4$		$CaWO_4$		$SrWO_4$		$PbWO_4$	
	B	B'	B	B'	B	B'	B	B'
Expt. (300 K)	52(5)	5(1)	74(7)	5.6(9)	63(7)	5.2(9)	66(5)	5.6(9)
Calc. (0 K)	55.8(8)	4.4(1)	80.1(5)	4.5(1)	69.9(2)	4.5(3)	61.7(7)	5.1(1)
Calc. (300 K)	46.8(4)	4.4	62.1(4)	4.5	56.3(6)	4.5	49.8(3)	5.1

(inset of Fig. 8). However, further increase in pressure beyond a threshold of 45 GPa leads to an abrupt increase in the W-O bond by about 0.1 Å. Hence it can be inferred that WO_4 tetrahedra are almost immune to changes in pressure up to an upper threshold of pressure, whose value is different for each of the tungstates. Beyond this threshold, WO_4 tetrahedra distort and the W atom's coordination increases.

Our above-said observations are in tandem with experimentally [24] observed amorphization around 45 GPa in $BaWO_4$ and at around 40 GPa in $CaWO_4$ [28]. The equation of state for various compounds has also been obtained (Fig. 4) from minimization of the enthalpy at 0 K. Table I gives the bulk modulus and its pressure derivative for the four compounds in comparison with the available reported experimental data [24]. The values are obtained from fitting of the Birch equation of state [46] to the calculated equation of states.

Earlier studies [23] surmise that a large ratio of ionic radii (WO_4/A) accommodates increased stresses through larger and more varied displacement from their average positions. This results in the loss of translational periodicity at high pressure. The larger the WO_4/A ratio, the lower the pressure threshold for pressure-induced amorphization. This

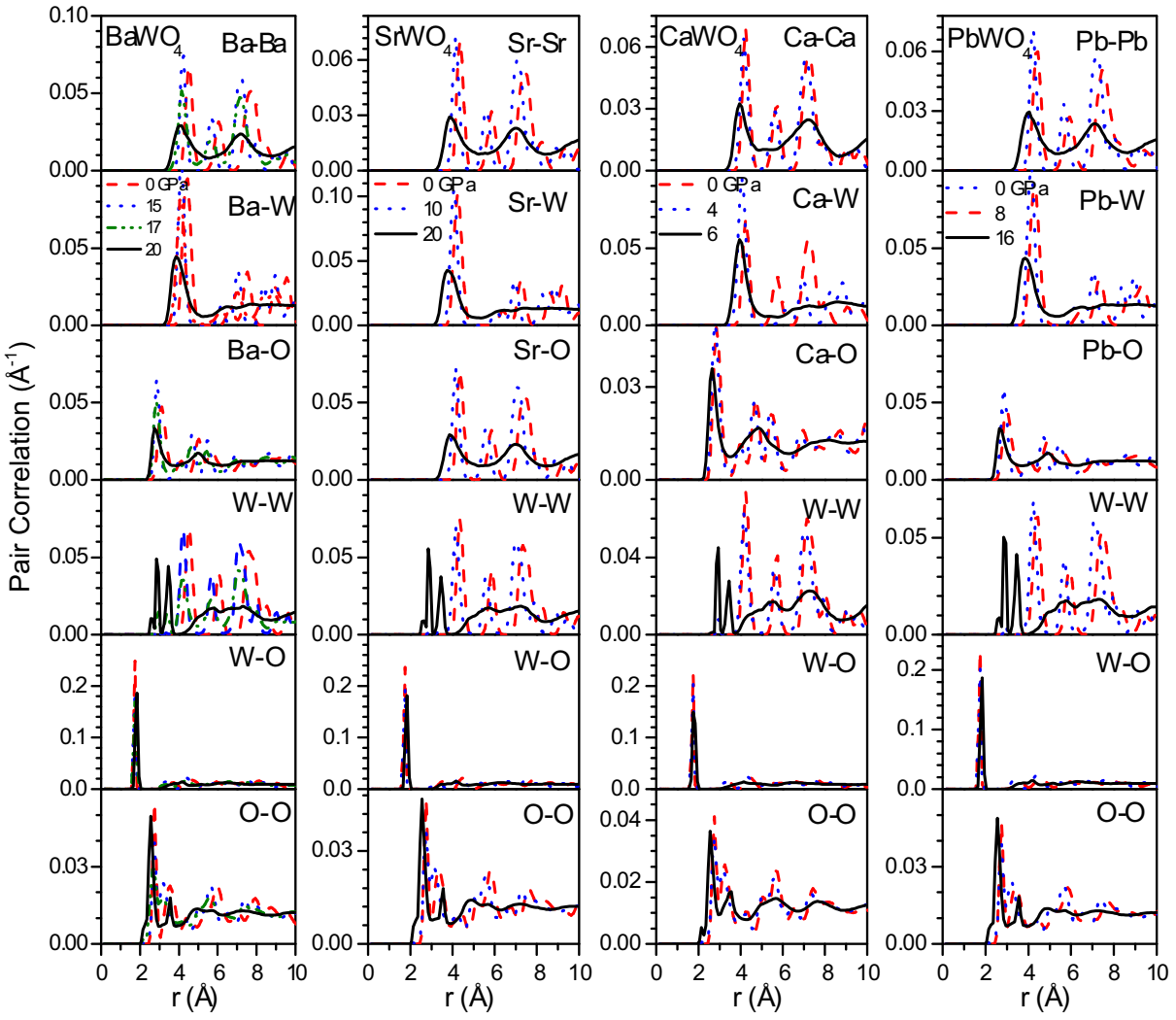

FIG. 9. (Color online) Pair correlations in the four tungstates at 700 K with increasing pressure (in GPa) as obtained from molecular dynamics simulations.

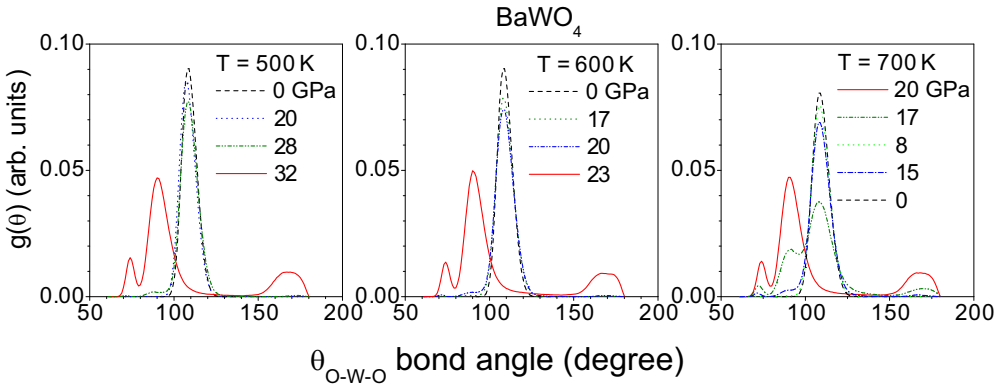

FIG. 10. (Color online) Intratetrahedral bond angle O-W-O correlation with increasing pressures in $BaWO_4$ at different temperatures.

ratio decreases according to the following order: $WO_4/Ca > WO_4/Sr > WO_4/Pb > WO_4/Ba$. According to this notion, $CaWO_4$ should have the lowest value of pressure for amorphization to occur, followed by $SrWO_4$, $PbWO_4$, and $BaWO_4$ respectively. Our computed results are in full agreement with this expected trend.

We have also studied the high-temperature, high-pressure response of the compounds. The pressure evolution of $BaWO_4$ has been studied at 500, 600, and 700 K. At these temperatures, we find that the compound exhibits amorphization at lower pressures in comparison to the calculations carried out at ambient temperature. At 500 K, $BaWO_4$ amorphizes at 32 GPa, at 600 K the signature of amorphization is evident at 23 GPa, and at 700 K, it is observed at 20 GPa. Hence application of temperature with increasing pressure speeds up the gradual readjustment of the polyhedra, eventually leading up to the loss of long-range order. Pressure evolutions of $SrWO_4$, $CaWO_4$, and $PbWO_4$ at 700 K were studied. It is found that all the compounds show early set-in of amorphization. Figure 9 gives the pair-correlation functions of different atom pairs in the four compounds. Figure 10 gives the angle correlation of O-W-O angle with increasing pressure in the compounds. It can be noted that in the case of $CaWO_4$ amorphization occurs at around 6 GPa, in $SrWO_4$ it occurs around 14 GPa, and in $PbWO_4$ it occurs at about 16 GPa at 700 K.

Errandonea *et al.* have carried out ADXRD, XANES, and *ab initio* studies [24–26] on the high-pressure transformations in $BaWO_4$ and $PbWO_4$. According to their studies, fergusonite is a metastable phase which is energetically and structurally very close to the ambient scheelite phase. The kinetically hindered monoclinic $P2_1/c$ phase is a first-order reconstructive sluggish transformation, which occurs due to the monoclinic distortion of the fergusonite lattice. In the $P2_1/c$ phase, W occurs in a distorted octahedral coordination, WO_6. As mentioned in Sec. III, we have carried out classical molecular dynamics calculations using a supercell consisting of $8 \times 8 \times 4$ unit cells (6144 atoms) to study the response of the compounds on compression at different temperatures. Calculations have been carried out from ambient pressure to around 50 GPa at room temperature, 500, 600, and 700 K. The equation of state has been integrated for about 1400 ps using a time step of 0.002 ps. We were unable to obtain any clear indications of the kinetically hindered phase [24–26] at the temperatures studied. Nevertheless, we found that the coordination of W is changing from 4 to 6, before final amorphization as reported by the above-said authors.

V. CONCLUSIONS

A combination of model and *ab initio* lattice dynamics has been used to study the vibrational properties in the four tungstates. Molecular dynamics simulations have been employed to understand their evolution with increasing pressure. Inelastic neutron scattering experiments have been carried out to measure the phonon density of states in the compounds. The calculations are in good agreement with experimentally measured data. With increasing pressure, tungstates undergo transition from scheelite to fergusonite phase; it is a second-order displacive transition with no apparent volume discontinuity. Enthalpy calculations using the *ab initio* method show that the scheelite to fergusonite transition is second order in nature. However, with further increase in pressure, these tungstates show pressure-induced loss of translational ordering, which is seen by the sudden drop in volume in all four tungstates studied, using molecular dynamics simulations. Under high temperature and high pressure, amorphization is found to occur at considerably lower pressure. On amorphization WO_4 tetrahedra deform, and the coordination of W atoms increases from 4. The AO_8 polyhedra show considerable distortion. The calculated amorphization pressures for $BaWO_4$ and $CaWO_4$ are in agreement with the available experimental data. The molecular dynamics simulations facilitate in predicting the amorphization in $SrWO_4$ and $PbWO_4$ at high pressures.

[1] D. Niermann, C. P. Grams, M. Schalenbach, P. Becker, L. Bohaty, J. Stein, M. Braden, and J. Hemberger, Phys. Rev. B **89**, 134412 (2014).

[2] M. Baum, J. Leist, Th. Finger, K. Schmalzl, A. Hiess, L. P. Regnault, P. Becker, L. Bohaty, G. Eckold, and M. Braden, Phys. Rev. B **89**, 144406 (2014).

[3] N. Poudel, K.-C. Liang, Y.-Q. Wang, Y. Y. Sun, B. Lorenz, F. Ye, J. A. Fernandez-Baca, and C. W. Chu, Phys. Rev. B **89**, 054414 (2014).

[4] I. V. Solovyev, Phys. Rev. B **87**, 144403 (2013).

[5] J. Ruiz-Fuertes, S. López-Moreno, J. López-Solano, D. Errandonea, A. Segura, R. Lacomba-Perales, A. Muñoz, S. Radescu, P. Rodríguez-Hernández, M. Gospodinov, L. L. Nagornaya, and C. Y. Tu, Phys. Rev. B **86**, 125202 (2012).

[6] J. Ruiz-Fuertes, A. Segura, F. Rodríguez, D. Errandonea, and M. N. Sanz-Ortiz, Phys. Rev. Lett. **108**, 166402 (2012).

[7] S. López-Moreno, P. Rodriguez-Hernandez, A. Munoz, A. H. Romero, and D. Errandonea, Phys. Rev. B **84**, 064108 (2011).

[8] J. Ruiz-Fuertes, D. Errandonea, S. López-Moreno, J. González, O. Gomis, R. Vilaplana, F. J. Manjón, A. Muñoz, P. Rodríguez-Hernández, A. Friedrich, I. A. Tupitsyna, and L. L. Nagornaya, Phys. Rev. B **83**, 214112 (2011).

[9] F. J. Manjon, J. López-Solano, S. Ray, O. Gomis, D. Santamaría-Pérez, M. Mollar, V. Panchal, D. Errandonea, P. Rodríguez-Hernandez, and A. Munoz, Phys. Rev. B **82**, 035212 (2010).

[10] J. Ruiz-Fuertes, D. Errandonea, R. Lacomba-Perales, A. Segura, J. González, F. Rodríguez, F. J. Manjon, S. Ray, P. Rodríguez-Hernández, A. Muñoz, Zh. Zhu, and C. Y. Tu, Phys. Rev. B **81**, 224115 (2010).

[11] R. Lacomba-Perales, D. Errandonea, D. Martinez-Garcia, P. Rodríguez-Hernandez, S. Radescu, A. Mujica, A. Muñoz, J. C. Chervin, and A. Polian, Phys. Rev. B **79**, 094105 (2009).

[12] R. Lacomba-Perales, D. Martinez-García, D. Errandonea, Y. Le Godec, J. Philippe, G. Le Marchand, J. C. Chervin, A. Polian, A. Múñoz, and J. López-Solano, Phys. Rev. B **81**, 144117 (2010); V. Panchal, N. Garg, A. K. Chauhan, Sangeeta, and S. M. Sharma, Solid State Commun. **130**, 203 (2004).

[13] D. Errandonea, J. Pellicer-Porres, F. J. Manjón, A. Segura, Ch. Ferrer-Roca, R. S. Kumar, O. Tschauner, P. Rodríguez-Hernández, J. López-Solano, S. Radescu, A. Mujica, A. Muñoz, and G. Aquilanti, Phys. Rev. B **72**, 174106 (2005).

[14] Y. Zhang, N. A. W. Holzwarth, and R. T. Williams, Phys. Rev. B **57**, 12738 (1998).

[15] R. Lacomba-Perales, D. Errandonea, A. Segura, J. Ruiz-Fuertes, P. Rdríguez-Hernandez, S. Radescu, J. López-Solano, A. Mujica, and A. Muñoz, J. Appl. Phys. **110**, 043703 (2011).

[16] A. A. Annenkov, M. V. Korzhik, and P. Lecoq, Nucl. Instrum. Methods Phys. Res., Sect. A **490**, 30 (2002).

[17] M. Nikl, P. Bohacek, E. Mihokova, N. Solovieva, A. Vedda, M. Martini G. P. Pazzi, P. Fabeni, M. Kobayashi, and M. Ishii, J. Appl. Phys. **91**, 5041 (2002).

[18] A. Brenier, G. Jia, and C. Y. Tu, J. Phys.: Condens. Matter **16**, 9103 (2004).

[19] H. E. Chao, Y. Kuisheng, L. Lei, and S. I. Zhenjun, J. Rare Earths **31**, 790 (2013).

[20] A Grzechnik, W. A Crichton, and M. Hanfled, Phys. Status Solidi **242**, 2795 (2005).

[21] J. López-Solano, P. Rodriguez Hernandez, S. Radescu, A. Mujica, A. Muñoz, D. Errandonea, F. J. Manjon, J. Pellicer Porres, N. Garro, A. Segura, Ch. Ferrer Roca, R. S. Kumar, O. Tschauner, and G. Aquilanti, Phys. Status Solidi B **244**, 325 (2007).

[22] F. J. Manjon, D. Errandonea, J. López-Solano, P. Rodríguez Hernandez, S. Radescu, A. Mujica, A. Muñoz, N. Garro, J. Pellicer Porres, A. Segura, Ch. Ferrer Roca, R. S. Kumar, O. Tschauner, and G. Aquilanti, Phys. Status Solidi B **244**, 295 (2007).

[23] F. J. Manjon and D. Errandonea, Prog. Mater. Sci. **53**, 711 (2008), and references therein. P. Blanchfield and G. A. Saunders, J. Phys. C: Solid State Phys. **12**, 4673 (1979).

[24] D. Errandonea, J. Pellicer-Porres, F. J. Manjón, A. Segura, C. Ferrer-Roca, R. S. Kumar, O. Tschauner, J. López-Solano, P. Rodríguez-Hernández, S. Radescu, A. Mujica, A. Muñoz, and G. Aquilanti, Phys. Rev. B **73**, 224103 (2006), and references therein.

[25] F. J. Manjon, D. Errandonea, N. Garro, J. Pellicer-Porres, P. Rodríguez-Hernández, S. Radescu, J. López-Solano, A. Mujica, and A. Muñoz, Phys. Rev. B **74**, 144111 (2006).

[26] F. J. Manjon, D. Errandonea, N. Garro, J. Pellicer-Porres, J. López-Solano, P. Rodríguez-Hernandez, S. Radescu, A. Mujica, and A. Muñoz, Phys. Rev. B **74**, 144112 (2006).

[27] P. Rodriguez Hernandez, J. López-Solano S. Radescu, A. Mujica, A. Muñoz, D. Errandonea, F. J. Manjon, J. Pellicer Porres, A. Segura, Ch. Ferrer Roca, R. S. Kumar, O. Tschauner, and G. Aquilanti, J. Phys. Chem. Solids **67**, 2164 (2006).

[28] D. Errandonea, M. Somayazulu, and D. Hausermann, Phys. Status Solidi B **235**, 162 (2003).

[29] W. Sleight, Acta Crystallogr., Sect. B **28**, 2899 (1972).

[30] A. Jayaraman, B. Batlogg, and L. G. VanUitert, Phys. Rev. B **31**, 5423 (1985); **28**, 4774 (1983).

[31] P. J. Miller, R. K. Khanna, and E. R. Lippincott, J. Phys. Chem. Solids **34**, 533 (1973).

[32] P. Goel, R. Mittal, S. L. Chaplot, and A. K. Tyagi, Pramana **71**, 1135 (2008); P. Goel, R. Mittal, and S. L. Chaplot, J. Phys.: Conf. Ser. **377**, 012094 (2012); P. Goel, R. Mittal, M. K. Gupta, M. N. Rao, S. L. Chaplot, S. Rols, A. K. Tyagi, and Z. Petr, Chin. J. Phys. **49**, 308 (2011).

[33] D. L. Price and K. Skold, in *Methods of Experimental Physics: Neutron Scattering, Part A*, edited by K. Skold and D. L. Price (Academic Press, Orlando, FL, 1986), Vol. 23; J. M. Carpenter and D. L. Price, Phys. Rev. Lett. **54**, 441 (1985).

[34] A. Sjolander, Ark. Fys. **14**, 315 (1958).

[35] S. Baroni, P. Giannozzi, and A. Testa, Phys. Rev. Lett. **58**, 1861 (1987).

[36] G. Kresse and J. Furthmüller, Comput. Mater. Sci. **6**, 15 (1996).

[37] G. Kresse and D. Joubert, Phys. Rev. B **59**, 1758 (1999).

[38] H. J. Monkhorst and J. D. Pack, Phys. Rev. B **13**, 5188 (1976).

[39] J. P. Perdew, K. Burke, and M. Ernzerhof, Phys. Rev. Lett. **77**, 3865 (1996).

[40] K. Parlinksi, PHONON software, 2003.

[41] S. L. Chaplot, N. Choudhury, S. Ghose, M. N. Rao, R. Mittal, and K. N. Prabhatasree, Eur. J. Mineral. **14**, 291 (2002).

[42] R. Mittal, S. L. Chaplot, and N. Choudhury, Prog. Mater. Sci. **51**, 211 (2006).

[43] G. Venkatraman, L. Feldkamp, and V. C. Sahni, *Dynamics of Perfect Crystals* (MIT Press, Cambridge, 1975).

[44] S. L. Chaplot (unpublished).

[45] W. G. Lyon and W. F. Edgar, J. Chem. Phys. **49**, 3374 (1968).

[46] F. Birch, J. Geophys. Res. **57**, 227 (1952).